Advancing Neuroscience Diagnostics: A Hyperspectral Imaging System for Real-Time Biochemical Insights into Brain Tissue

Anam Toaha[a,b*], Pietro Ricci[a,b], Louis Chessel[c], Dorotea Nardini[a,b], Luca Giannoni[d], Ilias Tachtsidis[d], Francesco Pavone[a,b,e]

[a]Department of Physics and Astronomy, University of Florence, Italy; [b]European Laboratory for Non-linear Spectroscopy, Italy; [c]Polytech Lyon, France; [d]Department of Medical Physics and Biomedical Engineering, University College London, UK; [e] National Institute of Optics, National Research Council, Italy
**Corresponding author Email: ricci@lens.unifi.it*

Abstract: Here we present a hyperspectral imaging system designed for advancing the detection and diagnosis of brain tumors. We provide a comprehensive characterization of the system, which guarantees rapid spectral scanning, tunable wavelength selection, large field of view, high signal-to-noise ratio and spatio-temporal resolution.
Keywords: hyperspectral imaging, brain tumor detection, spectral tissue differentiation.

1. Introduction

Hyperspectral imaging (HSI) is emerging as a powerful tool for tumor detection and the monitoring of tissue metabolic and hemodynamic processes [1]. By capturing and analyzing a broad spectrum of light across numerous narrow wavelength bands, HSI provides high-resolution spectral information at each pixel, enabling precise tissue differentiation based on unique spectral signatures. One of its most significant advantages is its completely non-invasive nature, unlike many conventional diagnostic techniques [2]. This makes HSI particularly promising for brain tumor detection and diagnostics, offering detailed spatial mapping of tumor localization and tissue characteristics in both healthy and diseased conditions.

In this context, we introduce HyperProbe1.1 (HP1.1), an advanced version of the original HP1.0 system [3], developed as part of the EU-funded HyperProbe project. Designed for preclinical research, HP1.1 aims to refine HSI technology for clinical translation. The overarching goal of the HyperProbe consortium is to develop a compact, cost-effective prototype capable of assisting surgeons in real-time brain tumor navigation with high accuracy. Compared to its predecessor, HP1.1 offers an extended spectral range, improved signal-to-noise ratio (SNR), a larger field of view, customizable acquisition parameters, and enhanced system stability. A comprehensive characterization of HP1.1 was performed, assessing SNR, emitted power, spatiotemporal resolution, sensitivity, and reproducibility. Initial validation involved imaging aqueous fluorescein solutions, followed by successful tests on fresh ex vivo surgical biopsies. Additional experiments were conducted using plastic phantoms with varying absorption and scattering properties to further evaluate the system performances.

2. Materials and Methods

The HP1. 1 (Fig. 1) features a broadband plasma laser source (ISTEQ XWS-65, 250–2500 nm) coupled with a flexible wavelength selector (Spectrolight, FWS-Poly-CUS-10) for tunable selection (385–1015 nm) with adjustable bandwidth (3–15 nm) and a minimum step size of 1 nm. Broadband optical fibers (Avantes, FC-IR1000-1) connect the laser to the selector, transmitting light directly to the target. Images are captured by a CMOS camera (PCO, pco.panda 4.2) with a 2048 × 2048 pixel sensor, an 80% peak quantum efficiency in the visible-NIR range, and a 40fps frame rate. The system scans the full 385–1015 nm range (127 bands, 5 nm steps) in under 25 seconds—fast enough to prevent tissue degradation. Hyperspectral scanning and acquisition are managed via a LabVIEW-based interface.

We probe the system with a glioma sample, obtained from neurosurgical procedures at Azienda Ospedaliero-Universitaria Careggi (Florence) with ethical approval (Studio ID: 23672-23672-BIO) and patient consent. It was washed in PBS to remove impurities, covered with a glass coverslip for a flat surface, and imaged within an hour post-surgery. System characterization includes testing on plastic phantoms (MEDPHOT matrix, BioPixs) and fluorescein (Sigma-Aldrich) detection from aqueous solutions at varying concentrations. A dark absorber was placed beneath the sample to prevent reflection, and acquisitions were performed in dark conditions. The reflectance spectrum from selected ROIs was calculated by removing background noise and normalizing against a white reference

(Labsphere, Spectralon® 5″). Sample attenuation (A) was determined using A = -log10R, where R is the average reflectance.

a)

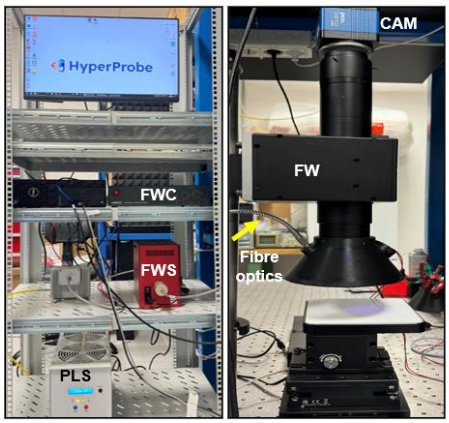

b)

Component	Manufacturer & model	Key specifics
PLS	Isteq, XWS-65	Broadband illumination (250-2500 nm); Spectral radiance up to 68 mW·m^{-2}·sr^{-1}·nm^{-1}; Output power stability less than 0.15%;
FWS	Spectrolight, FWS-Poly-CUS-10	Broadband selection (385-1015 nm); Variable bandwidth selection (3-15 nm); Band switching time between 10 and 100 ms;
Camera	PCO, pco.panda 4.2	4.2-MP (2048 x 2048) sensor; 6.5-µm pixel size; QE up to 80% (Visible and NIR); Maximum frame rate of 40 fps;
Filter Wheel	Cairn Research, Dual OptoSpin32	Up to 10 filter allocations; Stepping time between filters of 40-70 ms;
Optic fibres	Avantes, FC-IR1000-1	Broadband coverage (350-2500 nm); 1-mm core diameter;
Objective 1	Olympus, SDF PLAPO 1X PF	1x apochromatic macro objective; FOV of 0.65x0.65 cm^2;

Fig.1. a) Pictures of HyperProbe1.1 back (left) and front (right) panel, with all its components; CAM: Camera; FW: filter wheel; FWC: filter wheel controller; FWS: flexible wavelength selector, PLS: plasma light source. b) Table with the summary of the details and technical specifications HyperProbe1.1 components.

3. Results and Discussion

In this study, we conducted a comprehensive characterization of HyperProbe1.1 (HP1.1) and compared its performance with its predecessor, HP1.0. One of the most significant upgrades is the extended spectral range, now spanning 385–1015 nm compared to the previous 510–900 nm. This broader range allows for the detection of crucial spectral features, including fluorescein absorption at 490 nm, hemoglobin derivatives at 430 nm, and water absorption at 975 nm (Fig. 2a). These improvements enhance the system's ability to differentiate tissue types, which is essential for applications in tumor detection and surgical guidance.

To evaluate system sensitivity, we analyzed aqueous fluorescein solutions at varying concentrations. As shown in Fig. 2b, the system effectively detects even highly diluted solutions, down to a 10% concentration, demonstrating its high sensitivity to subtle spectral changes. Additionally, the field of view (FOV) of HP1.1 (Fig. 2c) is significantly larger (0.65 × 0.65 cm²) compared to HP1.0 (0.9 × 0.9 mm², Fig. 2d). While this increased FOV provides enhanced spatial coverage, it comes at the cost of a reduced spatial resolution which is 15.63µm compared to 3.48µm in HP1.0. However, the measured resolution closely aligns with theoretical Rayleigh predictions across all wavelengths, and notably, the system exhibits superior clarity at shorter wavelengths, as illustrated in Fig. 2e.

Further validation was conducted using solid phantoms with well-defined optical properties (Fig. 2f). The system's quantitative reliability was confirmed through a linear correlation between mean reflected intensity and both absorption and scattering coefficients (Fig. 2g, 2h, 2j). Additionally, the absorption-to-scattering ratio was analyzed, reinforcing system linearity (Fig. 2i). A key observation was made when analyzing disc B3, which mimics biological tissue properties. As expected, increasing the bandwidth of illumination resulted in a higher mean intensity due to greater light collection, albeit with an associated increase in standard deviation due to spectral averaging effects (Fig. 2k). Moreover, the system demonstrated strong stability and reproducibility over time, as indicated by the nearly constant mean intensity of disc B3 over prolonged measurements (Fig. 2l).

4. Conclusions

Overall, HP1.1 demonstrates significant improvements over its predecessor, HP1.0., offering enhanced stability, an expanded wavelength range (57.5% wider), and a larger FOV, making it a promising tool for neurosurgical applications. The ability to detect key spectral features, such as fluorescein and oxy-deoxyhemoglobin peaks, will aid in distinguishing healthy from tumor tissue. Future applications include in vivo studies in murine brain tumor models under varying physiological conditions (e.g., hyperoxia, hypoxia, normoxia), further optimizing the system's performance.

This characterization provides crucial insights into the system's capabilities and limitations, supporting its development into a cost-effective, compact, and precise neuronavigational tool for clinical use.

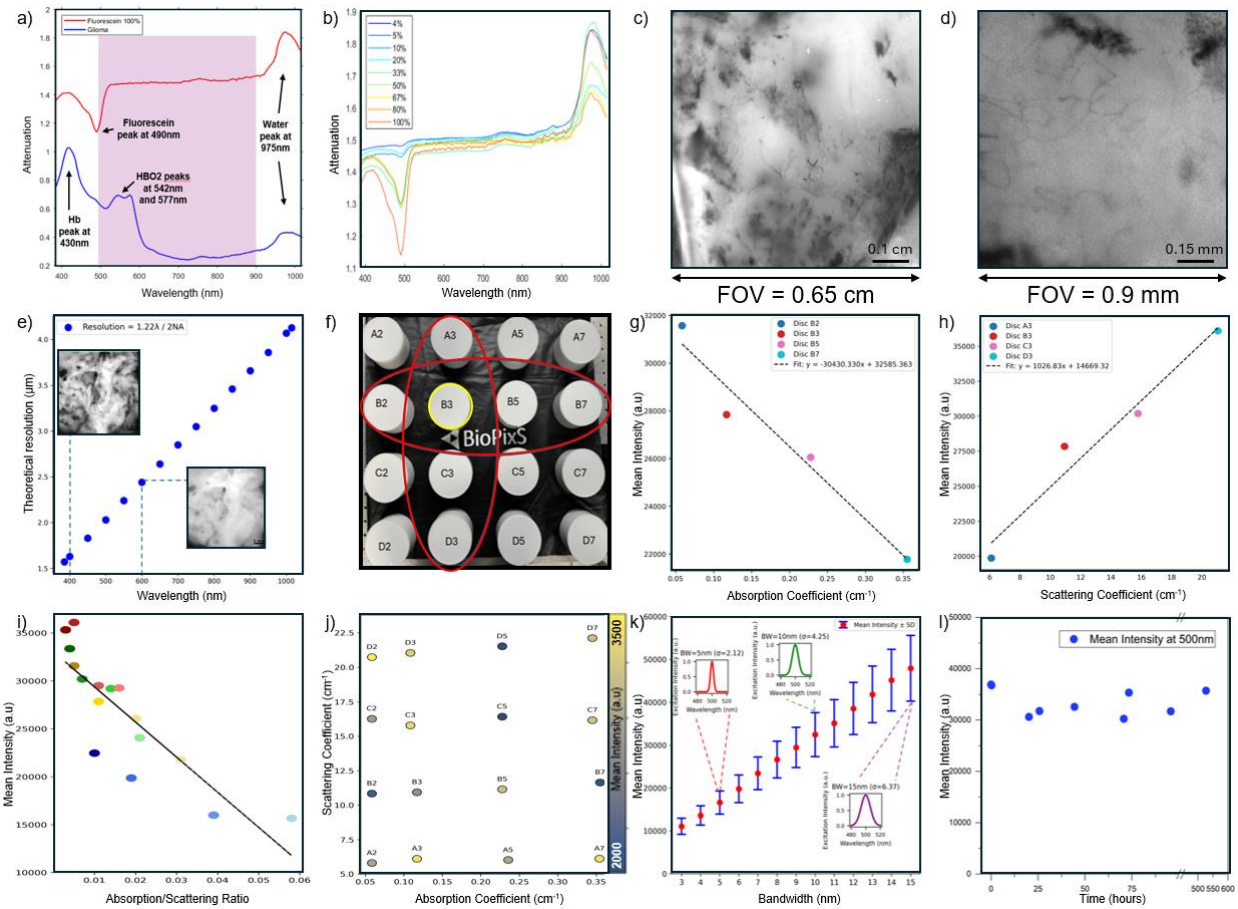

Fig.2. a) Attenuation spectra of a glioma tumor and fluorescein. The pink region indicates the limited spectral range of HP1.0. b) Attenuation spectra of fluorescein at different concentrations in water. c) and d) Glioma images taken with HP1.1 c) and HP1.0 d), respectively. e) Rayleigh's theoretical resolution and in insets, pictures of the glioma sample at 400 and 600nm. f) Picture of the MEDPHOT phantoms; Red ellipsoids indicate the plastic phantoms where the analysis has been conducted in g) and h); Yellow circle at disc B3; g) Mean reflected intensity in terms of absorption coefficients. h) Mean reflected intensity in terms of scattering coefficients. i) Mean reflected intensity as a function of the absorption coefficient/scattering coefficient for all sixteen discs. j) Mean reflected intensity as a function of the absorption coefficient and scattering coefficients for all sixteen discs. k) Mean intensity reflected from plastic phantom B3 at different bandwidths of illumination. Error bars are the standard deviation of the mean. In insets, normalised gaussian functions schematically representing the illumination width. l) Mean intensity reflected from discB3 as a function of time in hours.

5. Data Availability and Disclosures

The datasets generated during the current study are available from the corresponding author upon reasonable request. The authors declare no conflict of interest.

6. Acknowledgments

The HyperProbe consortium and project have received funding from the European Union's Horizon Europe research and innovation program under grant agreement No 101071040 – Project HyperProbe. Views and opinions expressed are however those of the author(s) only and do not necessarily reflect those of the European Union. Neither the European Union nor the granting authority can be held responsible for them. IT from UCL is supported by the UK Research and Innovation (UKRI) (Grant No. 10048387).

7.References

1. L. Giannoni, F. Lange, and I. Tachtsidis, "Hyperspectral imaging solutions for brain tissue metabolic and hemodynamic monitoring: Past, current and future developments," Journal of Optics (United Kingdom) 20, (2018).
2. S. Ortega, H. Fabelo, R. Camacho, M. de la Luz Plaza, G. M. Callicó, and R. Sarmiento, "Detecting brain tumor in pathological slides using hyperspectral imaging," Biomed Opt Express 9, 818 (2018).
3. L. Giannoni, M. Marradi, K. Scibilia, I. Ezhov, C. Bonaudo, A. Artemiou, A. Toaha, F. Lange, C. Caredda, B. Montcel, A. Della Puppa, I. Tachtsidis, D. Rückert, and F. S. Pavone, "Transportable hyperspectral imaging setup based on fast, high-density spectral scanning for in situ quantitative biochemical mapping of fresh tissue biopsies," J Biomed Opt 29, (2024).